

## Λ polarization in peripheral heavy ion collisions

F. Becattini,<sup>1,2</sup> L. P. Csernai,<sup>3</sup> and D. J. Wang<sup>3,4</sup>

<sup>1</sup>University of Florence and INFN Florence, Florence, Italy

<sup>2</sup>Frankfurt Institute for Advanced Studies (FIAS), Johann Wolfgang Goethe University, Frankfurt, Germany

<sup>3</sup>Institute of Physics and Technology, University of Bergen, Allegaten 55, 5007 Bergen, Norway

<sup>4</sup>Key Laboratory of Quark and Lepton Physics (MOE) and Institute of Particle Physics, Central China Normal University, Wuhan 430079, China

(Received 15 April 2013; revised manuscript received 11 July 2013; published 13 September 2013)

We predict the polarization of  $\Lambda$  and  $\bar{\Lambda}$  hyperons in peripheral heavy ion collisions at ultrarelativistic energy, based on the assumption of local thermodynamical equilibrium at the freeze-out. The polarization vector is proportional to the curl of the inverse temperature four-vector field and its length, of the order of percents, is maximal for a particle with moderately high momentum lying on the reaction plane. A selective measurement of these particles could make  $\Lambda$  polarization detectable.

DOI: [10.1103/PhysRevC.88.034905](https://doi.org/10.1103/PhysRevC.88.034905)

PACS number(s): 25.75.-q, 24.70.+s, 47.32.Ef

### I. INTRODUCTION

In peripheral high energy heavy ion collisions the system has a large angular momentum [1]. It has been recently shown in hydrodynamical computation that this leads to a large shear and vorticity [2]. When the quark-gluon plasma (QGP) is formed with low viscosity [3], interesting new phenomena may occur like rotation [4], or even turbulence, in the form of a starting Kelvin-Helmholtz instability (KHI) [5,6], or other turbulent phenomena [7]. Furthermore, the large angular momentum may manifest itself in the polarization of secondary produced particles [1,8,9]. Recently, a formula for the polarization of weakly interacting particles with spin 1/2 at local thermodynamical equilibrium has been found in Ref. [10] based on the extension of the Cooper-Frye formula to particles with spin. Provided that spin degrees of freedom equilibrate locally, the polarization turns out to be proportional to the vorticity of the inverse temperature four-vector field and can thus be predicted in a full hydrodynamical calculation of the collision process ended by the Cooper-Frye freeze-out prescription.

Early measurements of the  $\Lambda$  hyperon polarization [11], averaged over a significantly large centrality range, indicated relatively small values, with an upper bound  $|P_{\Lambda, \bar{\Lambda}}| \leq 0.02$  averaging over all azimuthal angles of  $\Lambda$  momentum. In this paper, we present a quantitative prediction of the  $\Lambda$ ,  $\bar{\Lambda}$  polarization, within a specific hydrodynamical calculation, at different centralities and its momentum dependence. At the top RHIC energy ( $\sqrt{s_{NN}} = 200$  GeV), although the resulting polarization is of the order of 1 to 2% on average, thus consistent with experimental bounds, it turns out to be the largest (around 7 to 9%) for hyperons with moderately high momentum lying in the reaction plane. A selective measurement of  $\Lambda$ 's with a few GeV momentum into the reaction plane could thus be able to show a finite polarization value, demonstrating that also spin degrees of freedom achieve local equilibrium and, in an indirect way, that vorticious flow is generated in peripheral heavy ion collisions.

The  $\Lambda$  polarization arising from this pure thermomechanical effect (spin degrees of freedom equilibration due

to the equipartition principle, as mentioned in the abstract) in principle competes with the polarization induced by the electromagnetic fields with the distinctive feature that the polarization vector induced by vorticity has the same orientation for particle and antiparticle, unlike for that induced by electromagnetic fields. However, at the freeze-out stage, the magnetic field produced by the moving spectators is estimated to be of the order of  $2 \times 10^{10}$  T [12] at  $\sqrt{s_{NN}} = 200$  GeV so that the resulting polarization is of the order of  $\mu_N g_{\Lambda} B/T \approx 10^{-6}$ , i.e., at least four orders of magnitude less than our predicted value. The polarization of  $\Lambda$  hyperons has been approached with different models (e.g., [8,13]). Recently, Ref. [14] has considered the local polarization of fermions in the plasma phase induced by the chiral anomaly, thus far with an unspecified transferring mechanism to final hadrons. We stress that in our approach the polarization of the observable hadrons is a consequence of the paradigm of local thermodynamical equilibrium; to be effective, the chiral anomaly should induce a modification of the velocity and temperature fields at the freeze-out.

### II. POLARIZATION

The  $\Lambda$  polarization in the participant center-of-mass frame, as a function of its momentum, reads (in units  $c = K = 1$ ) [10]:

$$\Pi_{\mu}(p) = \hbar \epsilon_{\mu\rho\sigma\tau} \frac{p^{\tau} \int d\Sigma_{\lambda} p^{\lambda} n_F (1 - n_F) \partial^{\rho} \beta^{\sigma}}{8m \int d\Sigma_{\lambda} p^{\lambda} n_F}, \quad (1)$$

where  $\beta^{\mu}(x) = [1/T(x)]u^{\mu}(x)$  is the inverse temperature four-vector field, and  $n_F$  is the Fermi-Jüttner distribution of the  $\Lambda$ , that is,  $1/(e^{\beta(x) \cdot p - \xi(x)} + 1)$ , being  $\xi(x) = \mu(x)/T(x)$  with  $\mu$  the relevant  $\Lambda$  chemical potential and  $p$  its four-momentum. Because at the temperatures typical of the freeze-out,  $\Lambda$  is quite dilute ( $m_{\Lambda} \gg T$ ), thus the Pauli blocking factor,  $(1 - n_F)$ , can be neglected in Eq. (1). The very same formula, with the replacement  $\xi \rightarrow -\xi$  applies to  $\bar{\Lambda}$ , namely, particles and

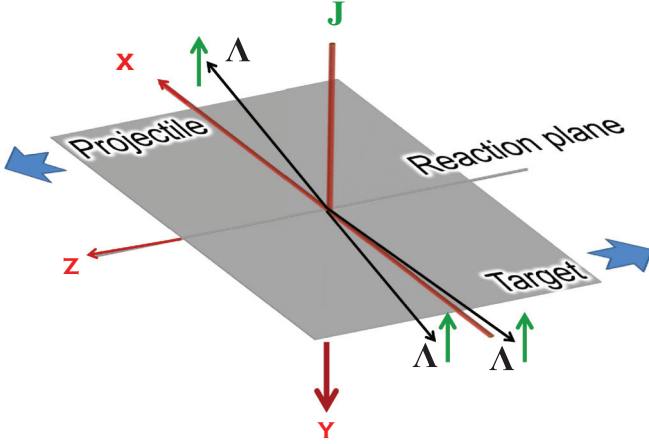


FIG. 1. (Color online) Sketch of peripheral heavy ion collisions at high energy. The  $\Lambda$  polarization points essentially into the direction of the total angular momentum ( $-y$ ) of the interaction region, orthogonal to the reaction plane.  $\Lambda$ 's with the largest polarization are emitted into the  $(xz)$  reaction plane.

antiparticles have the same polarization in the Boltzmann approximation.<sup>1</sup>

The polarization vector is then proportional to the antisymmetric part of the gradient of the inverse temperature field, henceforth defined as *thermal vorticity*:

$$\varpi^{\mu\nu} = \frac{1}{2}(\partial^\nu \beta^\mu - \partial^\mu \beta^\nu). \quad (2)$$

The spatial part of the polarization vector (1) gives rise to three terms:

$$\begin{aligned} \mathbf{\Pi}(p) = & \frac{\hbar \varepsilon}{8m} \frac{\int d\Sigma_\lambda p^\lambda n_F (\nabla \times \boldsymbol{\beta})}{\int d\Sigma_\lambda p^\lambda n_F} \\ & + \frac{\hbar \mathbf{p}}{8m} \times \frac{\int d\Sigma_\lambda p^\lambda n_F (\partial_t \boldsymbol{\beta} + \nabla \beta^0)}{\int d\Sigma_\lambda p^\lambda n_F}. \end{aligned} \quad (3)$$

The last two terms on the right hand side, involving polar vectors, should vanish because of the overall parity invariance (achieved combining symmetry by reflection with respect to the reaction plane of the two colliding nuclei and invariance by rotation of  $\pi$  around the axis orthogonal to the reaction plane). On the other hand, the first term, involving the spatial average of the curl of the  $\boldsymbol{\beta}$  field, which is an axial vector, is not ought to vanish; in fact it is a vector aligned with the total angular momentum direction, which is orthogonal to the reaction plane (see Fig. 1). It should be pointed out that these formulas apply to primary particles emitted from a locally equilibrated source. Secondary  $\Lambda$ 's emitted from either strong or weak decays—most likely—will have a lower polarization inherited from their parent particles.

In the simplest scenario of an isochronous ( $t = \text{const.}$ ) freeze-out at a given stage of the fluid dynamical expansion, according to the Cooper-Frye prescription,  $d\Sigma_\lambda p^\lambda \rightarrow dV \varepsilon$ ,  $\varepsilon = p^0$  being the  $\Lambda$ 's energy. In this case, the above formula

<sup>1</sup>Henceforth, unless otherwise stated, when referring to  $\Lambda$  we mean both particle and antiparticle states.

simplifies to

$$\mathbf{\Pi}(p) = \frac{\hbar \varepsilon}{8m} \frac{\int dV n_F (\nabla \times \boldsymbol{\beta})}{\int dV n_F}. \quad (4)$$

The  $\Lambda$  polarization is usually determined by measuring the angular distribution of the decay protons, which, in the  $\Lambda$  rest frame is given by

$$\frac{1}{N} \frac{dN}{d\Omega^*} = \frac{1}{4\pi} (1 + \alpha \mathbf{\Pi}_0 \cdot \hat{\mathbf{p}}^*),$$

where  $\alpha = 0.647$ ,  $\mathbf{\Pi}_0$  is the polarization vector, and  $\hat{\mathbf{p}}^*$  is the direction of the decay proton, both in the  $\Lambda$ 's rest frame. The vector  $\mathbf{\Pi}_0$  can thus be obtained by Lorentz boosting to this frame the one in Eq. (4):

$$\mathbf{\Pi}_0(p) = \mathbf{\Pi}(p) - \frac{\mathbf{p}}{\varepsilon(\varepsilon + m)} \mathbf{\Pi}(p) \cdot \mathbf{p}, \quad (5)$$

where  $(\varepsilon, \mathbf{p})$  is  $\Lambda$  four-momentum and  $m$  its mass. One can readily realize that  $\|\mathbf{\Pi}_0\| \leq \|\mathbf{\Pi}\|$  and equality is achieved only if either  $\mathbf{p} = 0$  (nonrelativistic limit) or when  $\mathbf{p} \cdot \mathbf{\Pi} = 0$ . In both cases, one has  $\mathbf{\Pi}_0(p) = \mathbf{\Pi}(p)$ . The above finding implies that maximal proper polarization of  $\Lambda$ 's with finite momentum is achieved when they are *transversely* polarized. Thus, if  $\mathbf{\Pi}$  is directed along the total angular momentum ( $-y$  direction in Fig. 1),  $\Lambda$ s having maximal polarization are those with momentum in the reaction plane or those with vanishing polar angle  $\theta$  (normally undetectable) and, in this case, their proper polarization vector is aligned with the total angular momentum.

### III. HYDRODYNAMICAL CALCULATION

The goal of the hydrodynamic calculation is to evaluate the thermal vorticity (2) at the freeze-out. In this paper we calculate it by using the particle in cell (PIC) fluid dynamic model, which provides us with the space-time development of the flow of the QGP. The freeze-out is enforced by means of the Cooper-Frye prescription at a fixed laboratory time  $t$ , such that the average temperature is  $\approx 180$  MeV (see below). In comparison with Ref. [2], only the relativistic case is considered.

For computational purposes, it is convenient to absorb the  $\hbar$  constant into  $\beta^\mu$  and redefine thermal vorticity as

$$\varpi^{\mu\nu} = \frac{1}{2}(\partial^\nu \hat{\beta}^\mu - \partial^\mu \hat{\beta}^\nu), \quad (6)$$

where  $\hat{\beta}^\mu \equiv \hbar \beta^\mu$ . Thereby,  $\varpi$  becomes dimensionless. Note that in the thermal vorticity definition there is no projection of the derivatives transverse to the flow (the operator  $\nabla_\mu = \partial_\mu - u_\mu u_\nu \partial^\nu$ ), unlike in the usual definition of the vorticity of the four-velocity field.

We present in Fig. 2 the  $zx$  component of the thermal vorticity weighted with the energy density in the cell [that is  $\Omega_{zx}(\text{cell}) = \varpi_{zx}(\text{cell}) \epsilon_{\text{cell}} / \langle \epsilon \rangle$ ] when the likewise weighted average temperature is 180 MeV, hence close to the freeze-out. The weighting with the energy density of the cell is described in detail in Ref. [2].

From Fig. 2 it can be seen that, at the last time step presented, in the reaction plane we have already an extended area occupied by matter. In the case of peripheral reactions

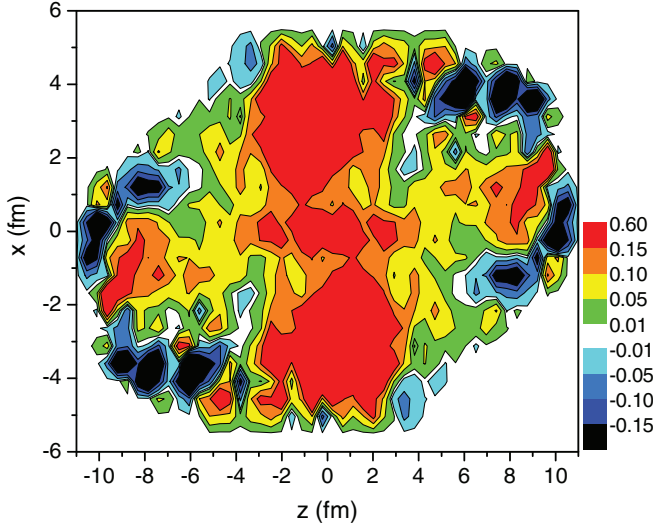


FIG. 2. (Color online) The energy density weighted thermal vorticity  $\Omega_{zx}(x, z)$  of the inverse temperature four-vector field  $\hat{\beta}^\mu$  (see text for definition) calculated for all  $[x - z]$  layers at  $t = 4.75$  fm/c, corresponding to an energy density weighted temperature of 180 MeV. The collision energy is  $\sqrt{s_{NN}} = 200$  GeV,  $b = 0.7 b_{max}$ . The cell size is  $dx = dy = dz = 0.4375$  fm, while the average weighted vorticity is  $\langle \Omega_{zx} \rangle = 0.0453$ . In most of the reaction plane, especially in the central regions the vorticity is positive, the forward and backward peripheral regions show smaller negative vorticities.

the multiplicity is relatively small, hence fluctuations in the reaction plane are considerable. In the relativistic case the outer edges show larger vorticity and random fluctuations are still strong. The average vorticity is smaller for the smaller impact parameters and it has positive value in the center and negative value at the edges.

It should be pointed out that while the standard velocity field vorticity rapidly decreases with expansion [2], thermal vorticity decrease is much slower and at some peripheral points it even increases. This is due to the fact that the matter cools during the expansion, so the temperature in the denominator of  $\beta^\mu$  decreases compensating for the decrease of the velocity field vorticity with time.

One should also mention that, in our calculation, hydrodynamical evolution starts after a dynamical longitudinal expansion based on collective Yang-Mills dynamics. The initial longitudinal size of the system is about  $2 \times 4$  fm, so the hydroprocess starts  $\approx 4$  fm/c after the interpenetration of the two Lorentz contracted nuclei. Consequently the configuration in Fig. 2 follows the interpenetration by about 8.5 fm/c, which is the time at which the energy density weighted average temperature is 180 MeV (see above).

#### IV. RESULTS AND DISCUSSION

The above described hydrodynamical calculation was performed for the conservative case presented in Fig. 2, which represents an initial rotation without the enhancement due to KHI. To calculate the average polarization of  $\Lambda$  hyperons,

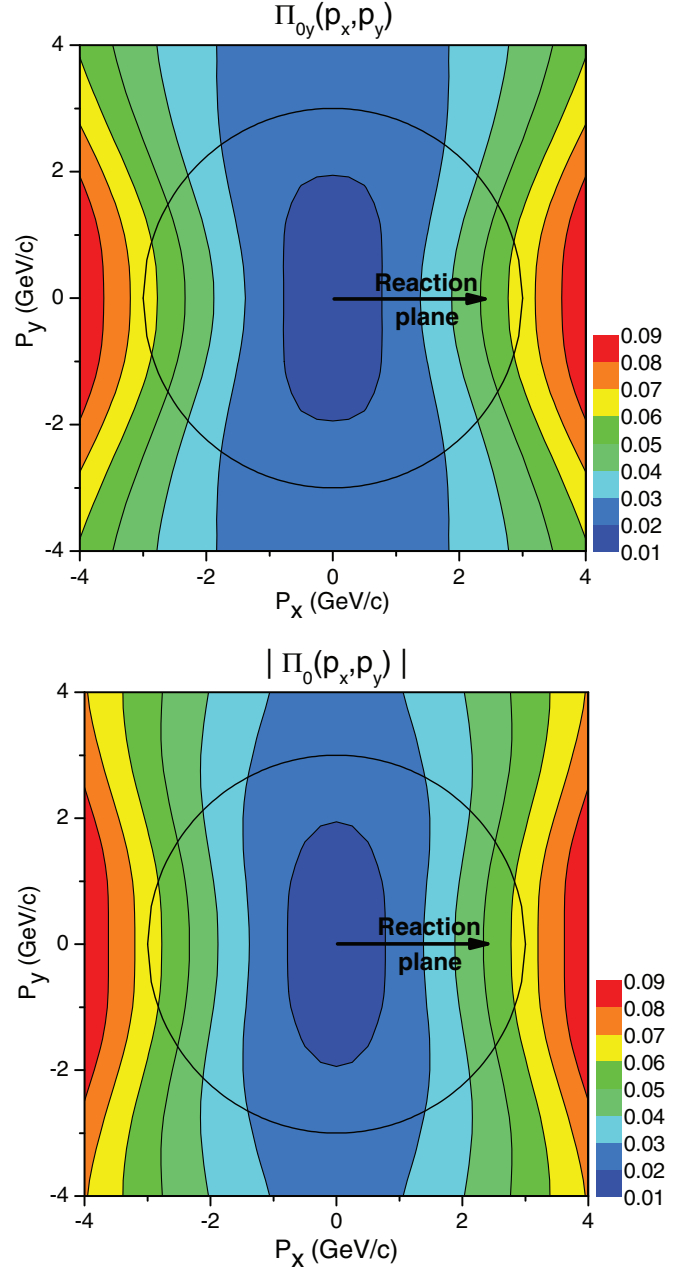


FIG. 3. (Color online) The dominant  $y$  component and the modulus of the observable polarization,  $\Pi_0(\mathbf{p})$  in the rest frame of the emitted  $\Lambda$ 's as a function of the  $\Lambda$  momentum in the transverse plane at the participant c.m. (i.e., at  $p_z = 0$ ). In the participant center of mass frame the polarization is minimal for small and  $y$  directed  $\Lambda$  momentum, while it is maximal in the  $x$  directed momentum, i.e., in the reaction plane.

the thermal vorticity has been properly weighted with the Fermi-Jüttner distribution  $n_F$ , according to Eq. (4).

The polarization vector, just as the flow vorticity, primarily points in the direction of the total angular momentum ( $-y$  in Fig. 1). It depends on the  $\Lambda$ 's momentum vector through the Fermi-Jüttner distribution  $n_F(\mathbf{p})$  [see Eq. (4)]. It increases with  $p_T$ , and it is also sensitive to the flow properties and

asymmetries; at  $\pm p_y \approx 3 \text{ GeV}/c$  it is about 2%, while in the reaction plane at  $p_x \approx 3 \text{ GeV}/c$  the polarization is about 5%. The proper polarization vector in the  $\Lambda$  rest frame, determining the decay products angular distribution therein, is related to the polarization vector in the collision frame by Eq. (5), which introduces a further dependence on the  $\Lambda$ 's direction, as has been mentioned. Note that Eq. (5) modifies the direction of  $\mathbf{\Pi}_0(p)$  with respect to  $\mathbf{\Pi}(p)$ , except in the case when either  $\mathbf{p}$  is lying on the reaction plane ( $p_y = 0$ ) or orthogonal to the reaction plane ( $p_{x,z} = 0$ ).

The numerical results for the magnitude of the proper polarization and its projection along the angular momentum axis  $y$  are shown in Fig. 3. It can be seen that both increase as a function of transverse momentum and that their maximum values are attained in the reaction plane ( $x$  direction). The average value of polarization is of the order of 1 to 2% (consistent with the RHIC bound), yet there are regions in momentum space where polarization is significantly larger and could be found with a selective measurement. The maximum up to  $p_T > 3 \text{ GeV}/c$  is around 5%, when  $\Lambda$ 's multiplicity is down by about two orders of magnitude compared to its top value, so that measuring polarization requires sufficiently large statistics. These results are significant even if our hydrodynamical model assumes the possible maximum initial angular momentum; other (still realistic) models may have 10 to 20% less, yet without strongly reducing the final polarization value. It should also be noted that the same hydro model shows the possible occurrence of the KHI, which enhance the effect by 10 to 20% [5].

It is important to stress that, in order to measure polarization, it is crucial to determine the orientation of the reaction plane, that is of the total angular momentum, on an event by event basis. As the polarization vector is oriented along the total angular momentum, a misidentification of the orientation would average to zero the measured polarization. A precise determination of the *direction* of the reaction plane is not as crucial because  $\Lambda$  polarization does not vary much in length and direction around it (being at a maximum; see Fig. 3). In order to improve accuracy, the participant center of mass (c.m.) should also be determined, both in pseudorapidity and in the transverse plane. This is usually not easy due to the limited acceptance of the central  $4\pi$  detectors, but can be done by using the zero degree calorimeters with adequate correction factors as shown in Ref. [15], for the longitudinal c.m. The same can be done in the transverse direction too.

A possible background to the sought signal of "hydrodynamical" polarization stems from polarized  $\Lambda$ 's emitted in single nucleon-nucleon ( $NN$ ) collisions at the outer edge of the overlap region of the two colliding nuclei (the so-called *corona effect*). It must be first pointed out that in  $NN$  collisions only  $\Lambda$ 's are found to be polarized whereas  $\bar{\Lambda}$ 's have a polarization consistent with zero. Since our predicted polarization applies to both particle and antiparticle states, a nonvanishing  $\bar{\Lambda}$  polarization would be free from this background. Nevertheless, we figure out that the  $NN$  background can be neglected also for  $\Lambda$  particle. Indeed, experimental observations show that  $\Lambda$ 's polarization scales with  $x_F \equiv 2p/\sqrt{s}$  [16], being  $p$  its momentum in the  $NN$  center-of-mass frame and that its magnitude strongly increases with  $x_F$  [17]. At very low

$x_F$ , where our calculation is performed (with  $y < 1$  and  $p_T$  up to 6 GeV, at the LHC energy scale of 1 TeV we have  $x_F \simeq 0.07$ ), the observed trend [18] indicates an approximate (generous) maximal polarization of 5% for  $p_T$  up to few GeVs. In order to estimate the impact of this background on the hydrodynamically originated polarization, one should estimate the number of single  $NN$  collisions in the corona as a function of the number of participants nucleons  $N_P$  in peripheral nuclear collisions. A calculation carried out by one of the authors [19] with the Glauber Monte-Carlo model at  $\sqrt{s_N}N = 200 \text{ GeV}$  shows that for peripheral collisions with  $N_P \simeq 100$  the number of nucleons undergoing single collisions in the corona is  $N_{PC} \simeq 30$ . According to a STAR measurement [20], for  $N_P \simeq 100$ , at midrapidity the  $\Lambda$  multiplicity is approximately  $3.6N_P$  times the one in  $pp$  collisions at the same energy. Therefore, the fraction of  $\Lambda$ 's coming from  $NN$  collisions with respect to the total production at  $N_P = 100$  can be estimated to be (see also Eq. (2) in Ref. [19])  $(N_{PC}/2)/(3.6N_P) = 15/360 \simeq 0.042$ . This implies that at the top RHIC energy, and even more so at the LHC energy where the fraction of corona collisions is lower, at most only about 4% of  $\Lambda$  hyperons come from  $NN$  collisions, and that their contribution to the measured polarization, at very low  $x_F$ , is at most  $0.04 \times 0.05 = 0.002$ , far below the signal level.

## V. CONCLUSIONS

In conclusion, we have predicted the polarization of  $\Lambda$  hyperons in relativistic heavy ion collisions at the RHIC energy and its momentum dependence. Our calculation did not include the polarization of secondary  $\Lambda$ 's from decays of resonances or  $\Xi$ s which, most likely, will tend to dilute the signal. Still, the polarization value may reach sizable and detectable values of several percent for momenta of some GeVs directed along the reaction plane. While the average value is predicted to be of the order of 1 to 2%, in agreement with the experimental bound previously set at the RHIC with about  $10^7$  minimum bias Au-Au events [11], with the much larger statistics (at least a factor of 30) collected by the RHIC in later runs [21], the momentum differential measurement of  $\Lambda$  and  $\bar{\Lambda}$  polarization in the direction along the reaction plane and at the participant c.m. should be feasible. We are also going to carry out similar calculations for the larger LHC energy.

The observation of a polarization arising from this thermomechanical effect of equipartition of angular momentum and in agreement with the predicted kinematic features would be a striking confirmation of the achievement of local thermodynamical equilibrium (for the spin degrees of freedom too) of the matter created in relativistic heavy ion collisions. It would also indicate that significant vorticity and circulation predicted in [4] may persist up to the freeze-out.

## ACKNOWLEDGMENT

This work was partly supported by Helmholtz International Center for FAIR. F.B., L.P.C., and D.J.W. would like to acknowledge the kind hospitality and thank for the enlightening discussions with the researchers of the Frankfurt Institute for Advanced Studies.

- [1] F. Becattini, F. Piccinini, and J. Rizzo, *Phys. Rev. C* **77**, 024906 (2008).
- [2] L. P. Csernai, V. K. Magas, and D. J. Wang, *Phys. Rev. C* **87**, 034906 (2013).
- [3] L. P. Csernai, J. I. Kapusta, and L. D. McLerran, *Phys. Rev. Lett.* **97**, 152303 (2006).
- [4] L. P. Csernai, V. K. Magas, H. Stöcker, and D. D. Strottman, *Phys. Rev. C* **84**, 024914 (2011).
- [5] L. P. Csernai, D. D. Strottman, and Cs. Anderlik, *Phys. Rev. C* **85**, 054901 (2012).
- [6] D. J. Wang, Z. Nédá, and L. P. Csernai, *Phys. Rev. C* **87**, 024908 (2013).
- [7] S. Floerchinger and U. A. Wiedemann, *J. High Energy Phys.* **11** (2011) 100; *J. Phys. G* **38**, 124171 (2011).
- [8] Z. T. Liang and X. N. Wang, *Phys. Rev. Lett.* **94**, 102301 (2005); **96**, 039901(E) (2006); J. H. Gao, S. W. Chen, W. T. Deng, Z. T. Liang, Q. Wang, and X. N. Wang, *Phys. Rev. C* **77**, 044902 (2008).
- [9] B. Betz, M. Gyulassy, and G. Torrieri, *Phys. Rev. C* **76**, 044901 (2007).
- [10] F. Becattini, V. Chandra, L. Del Zanna, and E. Grossi, *Ann. Phys.* **338**, 32 (2013).
- [11] STAR Collaboration, B. I. Abelev *et al.*, *Phys. Rev. C* **76**, 024915 (2007).
- [12] V. Voronyuk, V. D. Toneev, W. Cassing, E. L. Bratkovskaya, V. P. Konchakovski, and S. A. Voloshin, *Phys. Rev. C* **83**, 054911 (2011).
- [13] C. d. C. Barros, Jr., and Y. Hama, *Phys. Lett. B* **699**, 74 (2011).
- [14] J. H. Gao, Z. T. Liang, S. Pu, Q. Wang, and X. N. Wang, *Phys. Rev. Lett.* **109**, 232301 (2012).
- [15] L. P. Csernai, G. Eyyubova, and V. K. Magas, *Phys. Rev. C* **86**, 024912 (2012).
- [16] R608 Collaboration, A. M. Smith *et al.*, *Phys. Lett. B* **185**, 209 (1987).
- [17] B. Lundberg, R. Handler, L. Pondrom, M. Sheaff, C. Wilkinson, J. Dworkin, O. E. Overseth, R. Rameika, K. Heller, C. James *et al.*, *Phys. Rev. D* **40**, 3557 (1989).
- [18] M. Anselmino D. Boer, U. D'Alesio, and F. Murgia, *Czech. J. Phys.* **51**, A107 (2001).
- [19] F. Becattini and J. Manninen, *Phys. Lett. B* **673**, 19 (2009).
- [20] STAR Collaboration, B. I. Abelev *et al.*, *Phys. Rev. C* **77**, 044908 (2008).
- [21] See, e.g., [http://www.bnl.gov/rhic\\_aggs/users\\_meeting/agenda/Thurs/Gorbunov-STAR\\_Run\\_10.pdf](http://www.bnl.gov/rhic_aggs/users_meeting/agenda/Thurs/Gorbunov-STAR_Run_10.pdf).